11th International Conference on Vibration Problems
Z. Dimitrovová *et al.* (eds.)
Lisbon, Portugal, 9-12 September 2013

THE EFFECT OF INTERNAL FLOWING FLUID ON THE NON-LINEAR BEHAVIOR OF ORTHOTROPIC CIRCULAR CYLINDRICAL SHELLS

Zenon J. G. N. del Prado[*1,a], Ana Larissa D. P. Argenta[1,b], Frederico M. A. da Silva[1,c], Paulo B. Gonçalves[2]

[1]Federal University of Goiás
[a]zenon@eec.ufg.br, [b]analarissaargenta@hotmail.com, [c]silvafma@gmail.com

[2]Catholic University of Rio de Janeiro
paulo@puc-rio.br

Keywords: Cylindrical Shells, Orthotropic Material, Fluid-Structure Interaction, Non-linear Vibrations.

Abstract. *The great use of circular cylindrical shells for conveying fluid in modern industrial applications has made of them an important research area in applied mechanics. Many researchers have studied this problem, however just a reduced number of these works have as object the analysis of orthotropic shells. Although most investigations deal with the analysis of elastic isotropic shells in contact with internal and external quiescent or flowing fluid, several modern and natural materials display orthotropic properties and also stiffened cylindrical shells can be treated as equivalent uniform orthotropic shells. In this work, the influence of internal flowing fluid on the dynamic instability and non linear vibrations of a simply supported orthotropic circular cylindrical shell subjected to axial and lateral time-dependent loads is studied. To model the shell, the Donnell's non-linear shallow shell theory without considering the effect of shear deformation is used. A model with eight degrees of freedom is used to describe the lateral displacements of the shell. The fluid is assumed to be incompressible and non-viscous and the flow to be isentropic and irrotational. The Galerkin method is applied to derive the set of coupled non linear ordinary differential equations of motion which are, in turn, solved by the Runge-Kutta method. The obtained results show that the presence of the internal fluid and material properties have a great influence on the vibration characteristics of the shell.*

1 INTRODUCTION

Circular cylindrical shells are widely used structures in several engineering areas and their high efficiency as load carrying members for both axial loads and lateral pressure makes them the most common shell geometry for industrial applications. Cylindrical shells under a compressive stress state present usually a highly nonlinear behaviour under both static and dynamic loads and may exhibit several instability phenomena. The buckling and vibration analysis of cylindrical shells under various loading conditions is an important research area in applied mechanics mainly because these shells are widely used structures in several engineering areas and industrial applications. Also, the analysis of fluid-shell interaction has been a topic of continuous interest in the last decades. Most of the investigations are related to the analysis of elastic isotropic shells in contact with internal and external quiescent or flowing fluid. However, only a reduced number of investigations is concerned with the analysis of orthotropic shells.

Free vibrations of orthotropic cylindrical shells empty, partially or completely filled with an incompressible and non-viscous fluid have been studied by Jain [1], Warburton and Soni [2], Bradford and Dong [3], Chen *et al*. [4], among others. Selmane and Lakis [5] studied the influence of geometric nonlinearities associated with the shell and the fluid flow on the dynamics of empty and fluid filled elastic thin orthotropic cylindrical shells.

Del Prado *et al*. [6, 7, 8] using the Donnell's non-linear shallow shell theory without considering the effect of shear deformation, studied the influence of the ratio of Young's modulus in the circumferential and axial direction, on the non-linear vibrations of a simply supported fluid-filled orthotropic cylindrical shell, subjected to time-dependent loads. Recently, Amabili [9] using the Amabili-Reddy higher-order shear deformation theory studied the nonlinear dynamic behaviour of laminated circular cylindrical shells.

This work studies the non-linear vibrations of a simply supported orthotropic cylindrical shell with axial fluid flow and subjected to both axial time-dependent load and lateral harmonic pressure. To model the shell, the Donnell non-linear shallow shell theory without considering the effect of shear deformation is used. The fluid is assumed to be incompressible and inviscid and the flow to be isentropic and irrotational. The lateral displacements are described as a model with eight degrees of freedom, satisfying the relevant boundary and continuity conditions, and containing the fundamental, companion, gyroscopic and four axisymmetric modes and the Galerkin method is applied to derive a set of coupled non-linear ordinary differential equations of motion. The influence of both geometric parameters and material orthotropy on the non-linear dynamic response of the shell is studied. The obtained results show the marked influence of the orthotropic material properties, geometry, fluid flow and load parameters on the dynamic stability boundaries and resonance curves.

2 PROBLEM FORMULATION

In this work the mathematical formulation follows references [7, 8, 10, 11, 12]. Consider a simply supported cylindrical shell with radius R, thickness h, length L, containing an internal flowing fluid with velocity U and subjected to either a harmonic lateral pressure or a time-dependent axial load. In Figure 1 a simply supported cylindrical shell is displayed where the axial, circumferential and radial co-ordinates are denoted by x, $y=R\theta$ and z, respectively. The corresponding displacements of the shell middle surface are denoted by u, v and w. The middle surface of the shell is defined as the reference surface. It is assumed that the local coordinate system, which determines the principal axes of material orthotropy, coincides with the global cylindrical coordinates. The shell is made of an elastic orthotropic material with

Young's moduli E_{xx} and $E_{\theta\theta}$ in the axial and circumferential directions, respectively, shear modulus $G_{x\theta}$, Poisson coefficients ν_{xx} and $\nu_{\theta\theta}$, and mass density ρ_s.

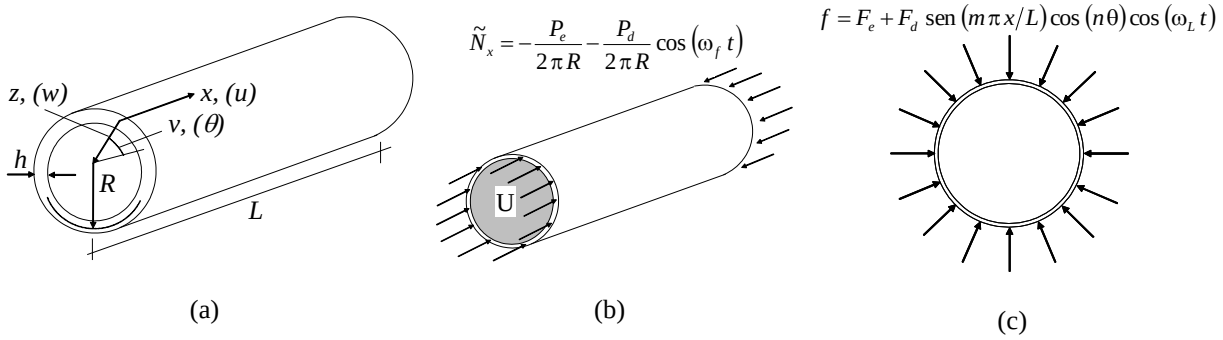

Figure 1: Shell characteristics. a) Shell geometry; b) axial harmonic load and fluid flow; c) harmonic lateral pressure.

For an orthotropic material, the extensional stiffness constants A_{ij} and the flexural stiffness constants D_{ij} are given by

$$A_{ij} = \int_{-h/2}^{h/2} Q_{ij}\, dz, \qquad D_{ij} = \int_{-h/2}^{h/2} Q_{ij}\, z^2\, dz\,, \tag{1}$$

with

$$Q_{11} = \frac{E_{xx}}{1-\nu_{xx}\nu_{\theta\theta}}, \qquad Q_{12} = Q_{21} = \frac{\nu_{xx}E_{\theta\theta}}{1-\nu_{xx}\nu_{\theta\theta}}, \qquad Q_{22} = \frac{E_{\theta\theta}}{1-\nu_{xx}\nu_{\theta\theta}}, \qquad Q_{33} = G_{x\theta}, \tag{2}$$

where because of symmetry, $E_{xx}\nu_{\theta\theta} = E_{\theta\theta}\nu_{xx}$.

The non-linear equation of motion based on the von Kármán-Donnell shallow shell theory, in terms of a stress function F and the lateral displacement w and disregarding the effect of shear deformations, is given by

$$\begin{aligned} &D_{11}\frac{\partial^4 w}{\partial x^4} + \frac{2}{R^2}\left(D_{12}+2D_{33}\right)\frac{\partial^4 w}{\partial x^2\partial\theta^2} + \frac{1}{R^4}D_{22}\frac{\partial^4 w}{\partial\theta^4} + c\,h\frac{\partial w}{\partial t} + \rho_S\,h\frac{\partial^2 w}{\partial t^2} = f - P_h + \frac{1}{R}\frac{\partial^2 F}{\partial x^2} + \\ &\frac{1}{R^2}\frac{\partial^2 F}{\partial\theta^2}\frac{\partial^2 w}{\partial x^2} - \frac{2}{R^2}\frac{\partial^2 F}{\partial x\partial\theta}\frac{\partial^2 w}{\partial x\partial\theta} + \frac{1}{R^2}\frac{\partial^2 F}{\partial x^2}\frac{\partial^2 w}{\partial\theta^2}, \end{aligned} \tag{3}$$

where c (kg/m^3 s) is the damping coefficient, the f and P_h are the radial pressures applied to the surface of the shell as a consequence of, respectively, external forces and the contained flowing fluid.

The compatibility equation is given by

$$P_{22}\frac{\partial^4 F}{\partial x^4} + \frac{1}{R^2}\left(P_{33}-2P_{12}\right)\frac{\partial^4 F}{\partial x^2\partial\theta^2} + \frac{1}{R^4}P_{11}\frac{\partial^4 F}{\partial\theta^4} = -\frac{1}{R}\frac{\partial^2 w}{\partial x^2} + \frac{1}{R^2}\left[\left(\frac{\partial^2 w}{\partial x\partial\theta}\right)^2 - \frac{\partial^2 w}{\partial x^2}\frac{\partial^2 w}{\partial\theta^2}\right], \tag{4}$$

where

$$P_{11} = \frac{A_{22}}{A_{11}A_{22}-A_{12}^2}, \qquad P_{12} = \frac{A_{12}}{A_{11}A_{22}-A_{12}^2}, \quad P_{22} = \frac{A_{11}}{A_{11}A_{22}-A_{12}^2}, \qquad P_{33} = \frac{1}{A_{33}}. \tag{5}$$

Using the stress function F, the forces in the axial, circumferential and tangential directions are [13]

$$N_{xx} = \frac{1}{R^2}\frac{\partial^2 F}{\partial \theta^2}, \qquad N_{\theta\theta} = \frac{\partial^2 F}{\partial x^2}, \qquad N_{x\theta} = -\frac{1}{R}\frac{\partial^2 F}{\partial x\, \partial \theta}\ . \tag{6}$$

The boundary conditions for the simply supported shell with the axial load $\tilde{N}_x(t)$ applied at $x = 0$ and $x = L$ are

$$w = 0, \quad M_{xx} = -\left[D_{11}\frac{\partial^2 w}{\partial x^2} + D_{12}\left(\frac{1}{R^2}\frac{\partial^2 w}{\partial \theta^2}\right)\right] = 0, \quad N_{xx} = \tilde{N}_x(t), \quad v = 0\,. \tag{7}$$

2.1 Expansion for the lateral displacement

The following modal expansion for the lateral displacements $w(x,\theta,t)$ in terms of the circumferential and axial variables is adopted [10]

$$\begin{aligned} w(x,\theta,t) &= \xi_{1,1}(t)\, h\, \sin(q)\cos(n\theta) + \xi_{1,1c}(t)\, h\, \sin(q)\sin(n\theta) + \xi_{1,2}(t)\, h\, \sin(2q)\cos(n\theta) \\ &+ \xi_{1,2c}(t)\, h\, \sin(2q)\sin(n\theta) + \xi_{0,1}(t) h\, \sin(q) + \xi_{0,3}(t) h\, \sin(3q) \\ &+ \xi_{0,5}(t) h\, \sin(5q) + \xi_{0,7}(t) h\, \sin(7q), \end{aligned} \tag{8}$$

where $\xi_{1,1}(t)$, $\xi_{1,1c}(t)$, $\xi_{1,2}(t)$, $\xi_{1,2c}(t)$, $\xi_{0,1}(t)$, $\xi_{0,3}(t)$, $\xi_{0,5}(t)$ and $\xi_{0,7}(t)$ are the time-dependent non-dimensional modal amplitudes, $q = m\pi x/L$ and m and n are, respectively, the number of half-waves in the axial direction and the number of waves in the circumferential direction. This modal expansion satisfies the out-of-plane boundary conditions and includes the basic vibration mode, the companion mode, gyroscopic modes and four axi-symmetric modes. The choice of these modes is based on previous investigations on modal solutions for the non-linear analysis of cylindrical shells [7, 11, 14, 15].

The solution for the stress function may be written as $F = F_h + F_p$, where F_h is the homogeneous solution and F_p, the particular solution. The particular solution F_p is obtained analytically by substituting the assumed form of the lateral deflection on the right-hand side of the compatibility equation, Eq. (4), and by solving the resulting linear partial differential equation together with the relevant boundary and continuity conditions.

The homogeneous part of the stress function can be written as

$$F_h = \frac{1}{2}\overline{N}_{xx} R^2 \theta^2 + \frac{1}{2}x^2\left\{\overline{N}_{\theta\theta} - \frac{1}{2\pi RL}\int_0^{2\pi}\int_0^{L}\frac{\partial^2 F_p}{\partial x^2} R\, d\theta\, dx\right\} - \overline{N}_{x\theta} R\theta, \tag{9}$$

where $\overline{N}_{xx}$, $\overline{N}_{\theta\theta}$ and $\overline{N}_{x\theta}$ are the average in-plane restraint stresses generated at the ends of the shell. This solution enables one to satisfy the in-plane boundary conditions on the average [10].

Boundary conditions allow us to express the in-plane restraint stresses $\overline{N}_{xx}$, $\overline{N}_{\theta\theta}$ and $\overline{N}_{x\theta}$ in terms of w and its derivatives as [12]

$$\overline{N}_{xx} = N_{xx}, \tag{10}$$

$$\overline{N}_{\theta\theta} = \frac{A_{12}}{A_{11}}\tilde{N}_x - \left(\frac{A_{12}^2 - A_{11}A_{22}}{A_{11}}\right)\frac{1}{2\pi}\int_0^{2\pi}\int_0^{L}\left[-\frac{w}{R} + \frac{1}{2}\left(\frac{1}{R}\frac{\partial w}{\partial \theta}\right)^2\right] dx\, d\theta, \tag{11}$$

$$\overline{N}_{x\theta} = 0 \tag{12}$$

Upon substituting the modal expressions for F and w into the equation of motion, Eq. (3), and applying the Galerkin method, a set of eight non-linear ordinary differential equations is obtained in terms of the time-dependent modal amplitudes $\xi(t)_{i,j}$.

2.2 Modelling of fluid-structure interaction

The fluid is assumed to be incompressible and inviscid and the flow to be isentropic and irrotational. To determine the perturbation pressure on the shell wall the Païdoussis and Denise [16] model is adopted. Following previous studies the perturbation pressure on the shell wall is found to be

$$P_h = \rho_F \frac{L}{m\pi} f_w \left(\frac{\partial^2 w}{\partial t^2} + 2U \frac{\partial^2 w}{\partial t \partial x} + U^2 \frac{\partial^2 w}{\partial x^2} \right), \tag{13}$$

where

$$f_w = \frac{1}{\dfrac{\mathrm{I}_n(n-1, m\pi R/L)}{\mathrm{I}_n^{'}(n, m\pi R/L)} - \dfrac{n}{m\pi R/L}}, \tag{14}$$

and ρ_F is the fluid density, U is the flow velocity, I_n is the nth order modified Bessel function and $\mathrm{I}_n^{'}$ is its derivative with respect to its argument.

3 NUMERICAL RESULTS

Consider a circular cylindrical shell with thickness $h = 0.002$ m, density mass $\rho_S = 7850$ kg/m^3 and density fluid $\rho_F = 1000$ kg/m^3. The damping coefficient is defined as $c = 2\zeta\rho_S\omega_0$, where ζ is the viscous damping factor and ω_0 is the natural frequency of the shell. In the present analysis, the adopted viscous damping factor is $\zeta = 0.009$. In the parametric analysis five different cases of orthotropic material [2, 17], with varying $E_{\theta\theta}/E_{xx}$ relations and Poisson ratios are adopted. Case 1 has the lowest $E_{\theta\theta}/E_{xx}$ relation while Case 5 has the highest $E_{\theta\theta}/E_{xx}$ relation, as shown in Table 1.

Case	ν_{xx}	$\nu_{\theta\theta}$	E_{xx} (10^{10} Pa)	$E_{\theta\theta}$ (10^{10} Pa)	$G_{x\theta}$ (10^{10} Pa)	$E_{\theta\theta}/E_{xx}$
1	0.131926	0.012114	22.7350	2.0876	0.7958	0.0918
2	0.131926	0.04	6.8599	2.0799	0.7958	0.3032
3	0.131926	0.131926	2.0545	2.0545	0.7958	1.0000
4	0.04	0.131926	2.0799	6.8599	0.7958	3.2982
5	0.012114	0.131926	2.0876	22.7350	0.7958	10.8905

Table 1: Shell physical properties.

To study the influence of the geometry on the behaviour of orthotropic shells, three different L/R ratios and three different R/h ratios were selected. Table 2 shows the geometries selected in this work.

L/R	R/h
1.75	800
	300
	75

Table 2: Selected shell geometries.

The following non-dimensional parameters are used for time, frequency, flow velocity, axial load and lateral pressure [7, 13]:

$$\tau = t\,\omega_0 \qquad \Omega = \frac{\omega}{\lambda}, \qquad \lambda = \sqrt{\frac{E_{xx}}{\rho_s R^2 \left(1-\nu_{xx}^2\right)}} \tag{15}$$

$$U_b = \frac{U}{V_a}, \qquad V_a = \frac{\pi^2}{L}\sqrt{\frac{E_{xx}\,h^2}{12\,\rho_s\left(1-\nu_{xx}^2\right)}} \qquad \Gamma_{0,1} = \frac{P_{e,d}}{P_{cr}}, \qquad P_{cr} = \frac{2\pi E_{xx}\,h^2}{\sqrt{3\left(1-\nu_{xx}^2\right)}} \tag{16}$$

$$\Lambda_{0,1} = \frac{F_{e,d}}{F_{cr}}, \qquad F_{cr} = \frac{E_{xx}\,h}{R}\left[\frac{\left((\pi R/L)^2+n^2\right)^2}{n^2}\,\frac{(h/R)^2}{12\left(1-\nu_{xx}^2\right)} + \frac{(\pi R/L)^4}{n^2\left((\pi R/L)^2+n^2\right)^2}\right] \tag{17}$$

Figure 2 shows the influence of the L/R and R/h ratios on the lowest natural frequency of a cylindrical shell and the associated number of circumferential waves (n) for the five orthotropy cases analyzed here. The L/R and R/h ratios influence directly the natural frequencies values and the number of circumferential waves. Shells with the same L/R and R/h ratios have the same lowest non-dimensional natural frequency and wavelength. As illustrated here, most shell geometries can be analyzed using Donnell's shallow shell theory ($n \geq 5$), however, depending on the material orthotropy and for low values of the R/h ratio, only short shells can be studied. For a given R/h ratio, Ω_0 and n decrease as L/R increases, and the shell tends to a long tube. For a given L/R, Ω_0 decreases as R/h increases.

Figure 3 shows the influence of the L/R and R/h ratios on the critical flow velocity of a cylindrical shell and the associated number of circumferential waves (n) for the five orthotropy cases analyzed here. As can be seen, L/R and R/h ratios influence directly the critical flow velocity of the shell as well as the circumferential wavenumber. Then for shells with both same L/R and R/h ratios, shells with low $E_{\theta\theta}/E_{xx}$ ratio will have lower critical flow velocities than shells with high $E_{\theta\theta}/E_{xx}$ ratio. As the value of the L/R ratio is increased, the critical flow velocity is also gradually increased.

Consider now a shell under dynamic axial load and varying frequency of excitation ω_f. Figure 4 and Figure 5 display the parametric instability boundaries for a slowly evolving system in the excitation frequency-excitation amplitude parameter control space with no static pre-load (P_e = 0.0), considering the five material cases and two geometric relations L/R = 1.75, R/h = 800 and L/R = 1.75, R/h = 75 for empty shell, fluid-filled shell and increasing of flow velocity. The parametric instability boundary is the limit where small perturbations from the trivial solution will result in an initial exponential growth in the oscillations, leading to an oscillatory response. This boundary is obtained by increasing slowly the excitation amplitude while holding the frequency constant. The parametric instability boundary is composed of various curves, each one associated with a particular bifurcation event. The first important instability region is associated with the direct resonance zone when the frequency of excitation is equal to the lowest natural frequency of the fluid-filled shell (ω_f/ω_0 = 1.0). The second well to the right is associated to the principal parametric instability region and oc-

curs when the frequency of excitation is equal to two times the lowest natural frequency of the fluid-filled shell ($\omega_f/\omega_0 = 2.0$).

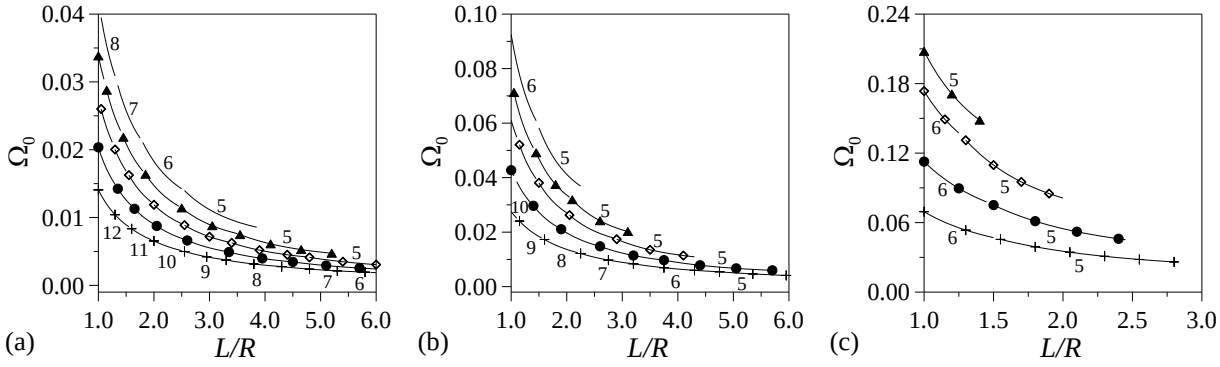

Figure 2: Variation of the lowest frequency parameter Ω_0 as a function of the shell geometric parameters L/R and R/h. (a) R/h = 800, (b) R/h = 300 e (c) R/h = 75. +—+—+ Case 1, ●—●—● Case 2, ◇—◇—◇ Case 3, ▲—▲—▲ Case 4, ——— Case 5.

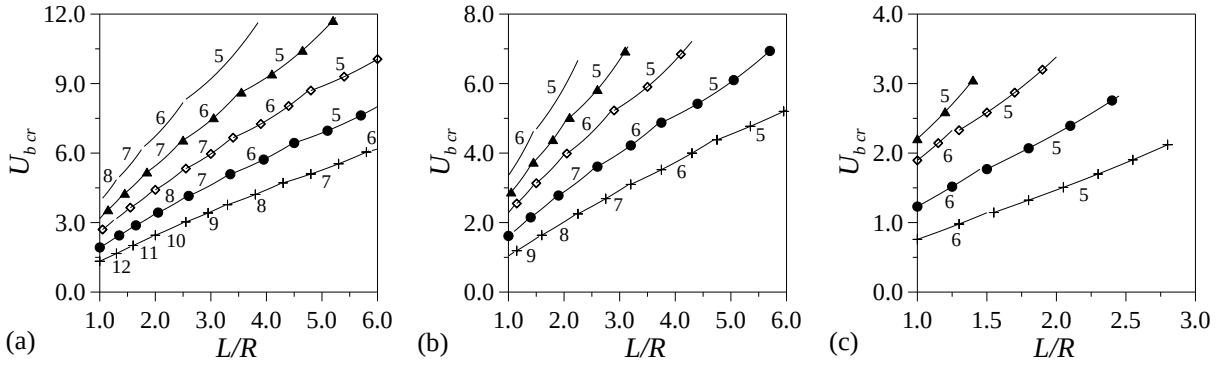

Figure 3: Variation of critical flow velocity $U_{b\,cr}$ as a function of the shell geometric parameters L/R and R/h. (a) R/h = 800, (b) R/h = 300 e (c) R/h = 75. +—+—+ Case 1, ●—●—● Case 2, ◇—◇—◇ Case 3, ▲—▲—▲ Case 4, ——— Case 5.

Figure 4 compares the instability boundaries of an empty shell, fluid filled shell ($U_b = 0$) and shells with increasing values of flow velocity. As observed, the material properties, flow velocity and geometric ratios strongly affect the instability boundaries. For an empty shell the instability boundaries display continuous lines and marked wells in first and second instability regions but, when fluid is considered (fluid filled or axial flow) there is a strong change on the boundaries and new discontinuities on the ascending and descending paths are displayed. When fluid is considered there is shifting to the left of all boundaries due to the reduction on the natural frequency of the shell. For shells with high $E_{\theta\theta}/E_{xx}$ relation the instability wells are deeper with high axial amplitude parameters than shells with low $E_{\theta\theta}/E_{xx}$ ratio.

Figure 5 displays the instability boundaries of an empty shell, fluid filled shell ($U_b = 0$) and shells with increasing values of flow velocity. As can be observed, even for an empty shell, the instability boundary displays discontinuities in the upper region between the two main regions and again, when fluid is considered, there is a shifting to the left of boundaries as well as the new discontinuities are observed.

Consider now a cylindrical shell subjected to harmonic lateral pressure with frequency ω_L. Figure 6 and Figure 7 display the comparison of resonance curves for and empty shell and a fluid-filled shell ($U_b = 0$) for geometric relations L/R = 1.75, R/h = 800, amplitude of lateral pressure parameter Λ_1 = 10% $\Lambda_{0\,cr}$ and considering three orthotropic materials (Case 1, Case 3

and Case 5). As can be observed, all empty cylindrical shells (Figures 6a, 6b and 6c) display softening behaviour with coexistence of both stable (continuous line) and unstable (dotted line) paths, also, for shells with high $E_{\theta\theta}/E_{xx}$ relation, a new stable branch initiates for high frequency pressure values. Now, when static fluid is considered (Figures 7a, 7b and 7c) the non-linear response of the shell changes completely. In Figure 7a for a shell with low $E_{\theta\theta}/E_{xx}$ relation, the softening behaviour is increased and chaotic vibrations can be observed. If $E_{\theta\theta}/E_{xx}$ relation is increased (Case 3 and Case 5), Figures 7b and 7c, also the softening response of the shell is increased and a new jump with stable paths are displayed.

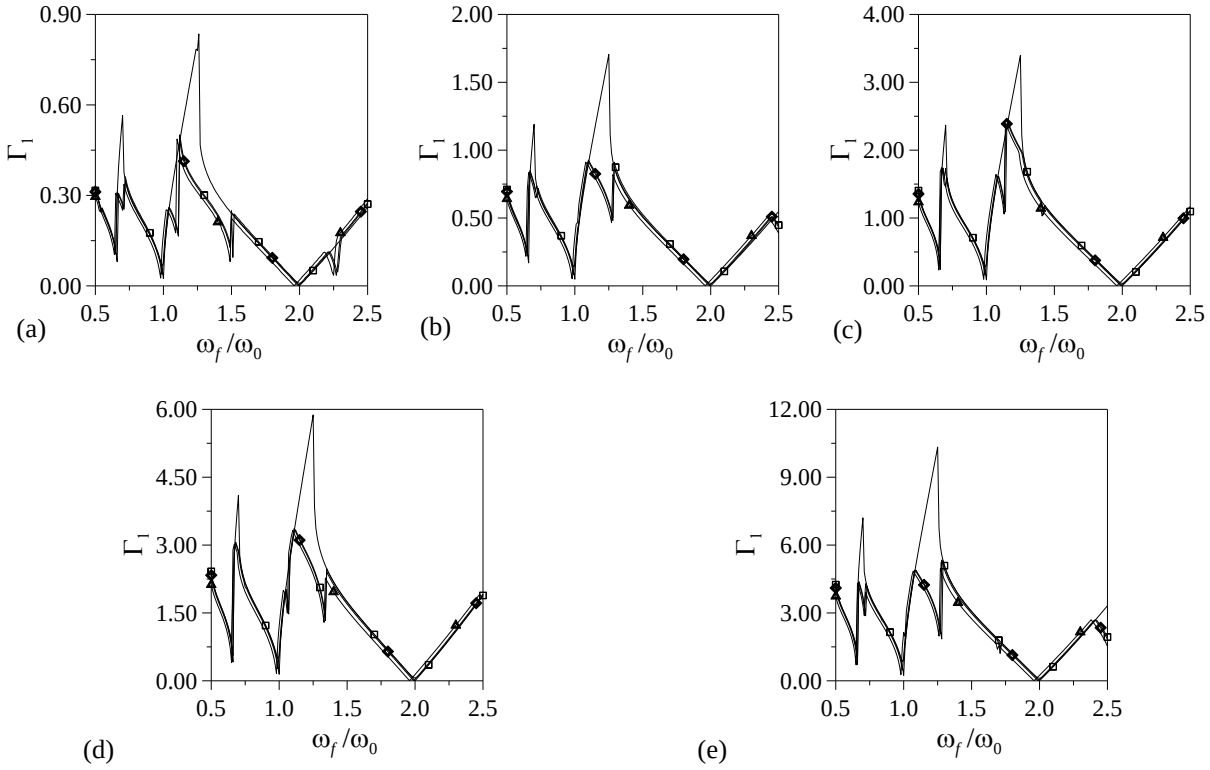

Figure 4: Parametric instability boundaries for harmonic axial load and L/R = 1.75 and R/h = 800. (a) Case 1, (b) Case 2, (c) Case 3, (d) Case 4 and (e) Case 5. ——— Empty shell, ▫—▫—▫ Fluid filled (U_b = 0), ◇—◇—◇ U_b = 10% $U_{b\,cr}$, ▵—▵—▵ U_b = 20% $U_{b\,cr}$.

4 CONCLUSIONS

- The influence of geometric and material characteristics on the linear and non-linear vibrations of simply supported orthotropic fluid-filled cylindrical shells subjected to axial and lateral time dependent loads is analyzed. To model the shell, the Donnell's non-linear shallow shell theory without considering the effect of shear deformation is used.
- Results show that the material orthotropy and L/R and R/h ratios have strong influence on the critical flow velocity and natural frequencies.
- For a harmonic axial load and harmonic lateral pressure both the parametric instability boundaries and resonance curves are strongly affected by geometric ratios, material properties and the presence of fluid displaying coexistence of chaotic, stable and unstable paths.

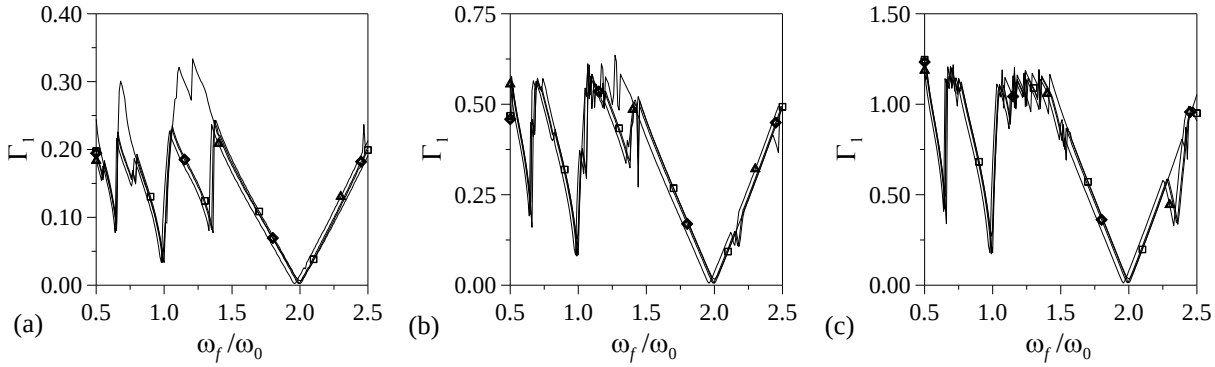

Figure 5: Parametric instability boundaries for harmonic axial load and L/R = 1.75 and R/h = 75. (a) Case 1, (b) Case 2 e (c) Case 3. ——— Empty shell, ▫—▫—▫ Fluid filled (U_b = 0), ◇—◇—◇ U_b = 10% $U_{b\,cr}$, △—△—△ U_b = 20% $U_{b\,cr}$.

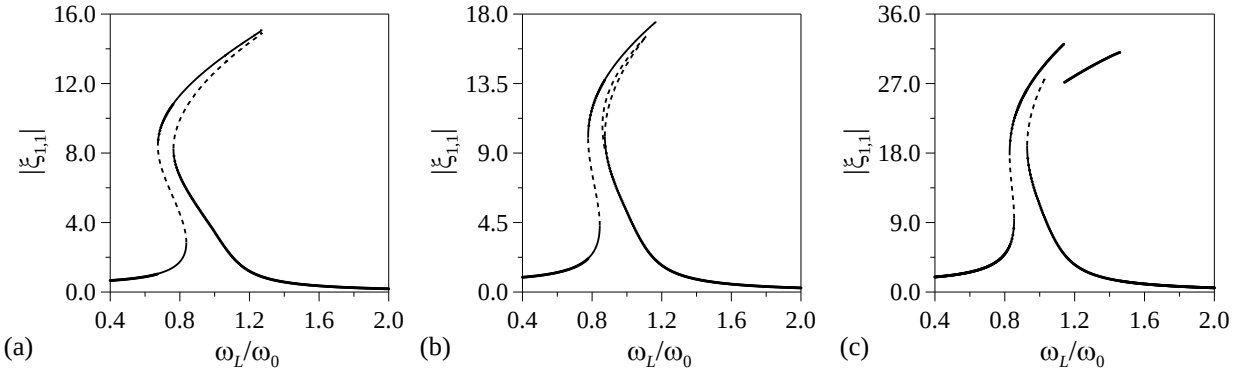

Figure 6: Resonance curves for an empty shell with lateral harmonic pressure for L/R = 1.75, R/h = 800 and Λ_1 = 10% $\Lambda_{0\,cr}$. (a) Case 1, (b) Case 3 and (c) Case 5.

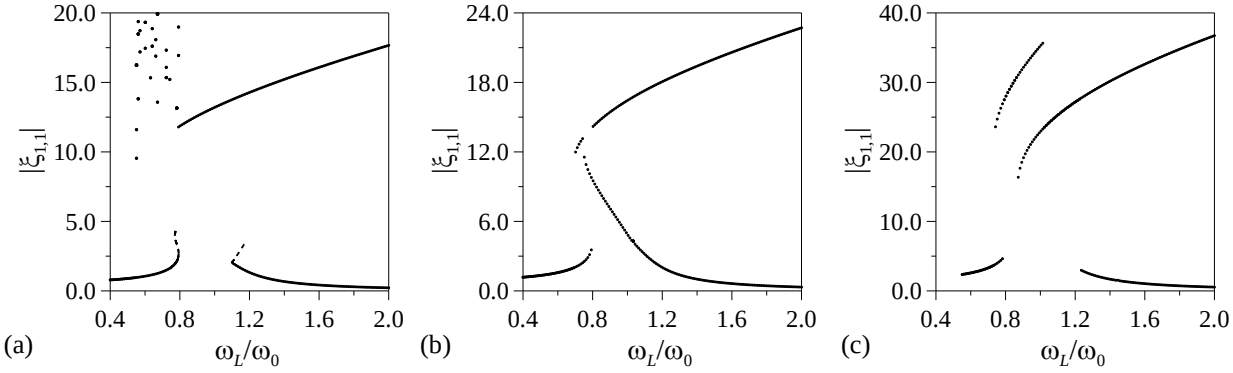

Figure 7: Resonance curves for a fluid filled shell with lateral harmonic pressure for L/R = 1.75, R/h = 800 and Λ_1 = 10% $\Lambda_{0\,cr}$. (a) Case 1, (b) Case 3 and (c) Case 5.

ACKNOWLEDGEMENTS

This work was made possible by the support of the Brazilian Ministry of Education – CAPES, CNPq and FAPERJ-CNE.

REFERENCES

[1] R.K. Jain, Vibration of fluid-filled, orthotropic cylindrical shells. *Journal of Sound and Vibration*, **37**, 379-388, 1974.

[2] G.B. Warburton, S.R. Soni, Resonant response of orthotropic cylindrical shells. *Journal of Sound and Vibration*, **53**, 1-23, 1977.

[3] L.G. Bradford, S.B. Dong, Lateral vibrations of orthotropic cylinders under initial stress. *Journal of Sound and Vibration*, **60**, 157-175, 1978.

[4] W.Q. Chen, H.J. Ding, Y.M. Guo, Q.D. Yang, Free vibrations of fluid-filled orthotropic cylindrical shells. *Journal of Engineering Mechanics*, **123**, 1130-1133, 1997.

[5] A. Selmane, A.A. Lakis, Non-linear dynamic analysis of orthotropic open cylindrical shells subjected to a flowing fluid. *Journal of Sound and Vibration*, **202**, 67-93, 1997.

[6] Z.J.G. del Prado, P.B. Gonçalves, M.P. Païdoussis, Dynamic instability of imperfect orthotropic cylindrical shells with internal flowing fluid. J. Ambrósio et al. eds. *7th EUROMECH Solid Mechanics Conference*, Lisbon, 1-15, 2009.

[7] Z.J. del Prado, P.B. Gonçalves, M.P. Païdoussis, Non-linear vibrations and instabilities of orthotropic cylindrical shells with internal flowing fluid. *International Journal of Mechanical Sciences*, **52**, 1437-1457, 2010.

[8] Z.J. del Prado, A.L.D.P. Argenta, F.M.A. Da Silva, P.B. Gonçalves. Dynamic instability of orthotropic cylindrical shells with internal flowing fluid and combined loads. *25th Conference on Noise and Vibration Engineering*, ISMA, Leuven, Belgium, 2012.

[9] M. Amabili, Nonlinear vibrations of laminated circular cylindrical shells: comparison of different shell theories. *Composite Structures*, **94**, 207-220, 2011.

[10] M. Amabili, F. Pellicano, M.P. Païdoussis, Non-linear dynamics and stability of circular cylindrical shells containing flowing fluid. Part I: Stability. Journal *of Sound and Vibration*, **225**, 655-699, 1999.

[11] P.B. Gonçalves, Z.J.G.N. del Prado, Non-linear oscillations and stability of parametrically excited cylindrical shells. *Meccanica*, **37**, 569-597, 2002.

[12] F. Pellicano, M. Amabili, Dynamic instability and chaos of empty and fluid-filled circular cylindrical shells under periodic axial loads. *Journal of Sound and Vibration*, **293**, 227-252, 2006.

[13] D.O. Brush, B.O. Almroth, *Buckling of Bars, Plates and Shells*. McGraw Hill Book Company, New York, 1975.

[14] P.B. Gonçalves, R.C. Batista, Non-linear vibration analysis of fluid-filled cylindrical shells. *Journal of Sound and Vibration*, **127**, 133-143, 1988.

[15] Z. del Prado, P.B. Gonçalves, M.P. Paidoussis, Non-linear vibrations and imperfection sensitivity of a cylindrical shell containing axial fluid flow. *Journal of Sound and Vibration*, **327**, 211-230, 2009.

[16] M.P. Païdoussis, *Fluid Structure Interactions*. Slender Structures and Axial Flow, Elsevier Academic Press, London, 2004.

[17] X. Li, Y. Chen, Transient dynamic response analysis of orthotropic circular cylindrical shell under external hydrostatic pressure. *Journal of Sound and Vibration*, **257**, No967-976, 2002.